Volume 19, Issue 2, 192528 (1-14)

Majlesi Journal of Electrical Engineering (MJEE)

https://doi.org/10.57647/j.mjee.2025.1902.28

Solar panel fault diagnosis based on the intelligent recursive method

Saadat Boulanouar*, Fengal Boualem

Faculty of Technology, University of Chlef 02000 DZ, Algeria.

*__Corresponding author:__ b.saadat@univ-chlef.dz

Original Research

Received:
24 January 2025
Revised:
5 March 2025
Accepted:
9 May 2025
Published online:
1 June 2025

Abstract:

The solar panel or solar cell is one of the most important components of the solar system that produces electrical energy with high efficiency compatible with electrical loads, but any defect in this cell can cause its efficiency to decrease. The objective of this work is to establish a fault diagnosis method that can be implemented in a real structure. These faults are diagnosed and located by implementing an algorithm based on the measured values of the solar panel using an intelligent recursive least squares approach. Our objective is to contribute to the diagnosis of faults in photovoltaic systems based on fuzzy logic in a recurrent manner. The integration of recursive least squares (RLS) with fuzzy logic are essential to improve system efficiency and reliability. This approach enables rapid identification and resolution of faults, helping to avoid energy losses, reduce downtime and support proactive maintenance. It guarantees the optimal functioning of solar panels, maximizing energy production and improving return on investment. Quantitatively, this method achieves high diagnostic accuracy (over 90%), reduces error rates by up to 30% under dynamic conditions, and provides real-time fault detection with minimal latency. The combination of RLS and fuzzy logic improves fault diagnosis by effectively handling uncertainties and handling ambiguous situations better than traditional methods.

Keywords: Solar panel; Fault diagnosis; Recursive least squares; Fuzzy logic

1. Introduction

Photovoltaic solar energy is a sustainable and non-polluting energy source. It plays a significant role in research to meet future energy needs. Currently, PV module manufacturing technology has evolved considerably in quality and production cost [1].
Defects in a photovoltaic installation can occur during its design, installation, and operation [2]. These defects decrease the performance of photovoltaic systems, affecting photovoltaic production [3].
The issue of diagnosing a solar panel using fuzzy logic aims to assess its operational state based on incomplete or uncertain data. Fuzzy logic allows for simulating how individuals make decisions in the face of uncertainty. In this context, the goal is to determine whether the panel is functioning correctly, if it has minor or major defects, or if it is completely out of service. By integrating fuzzy variables such as the panel's temperature, output voltage, and the amount of energy produced, fuzzy logic can provide a more accurate evaluation of the solar panel's condition.
The diagnostic approach for a solar panel using fuzzy logic, combined with recursive least squares optimization, represents a promising method for analyzing and resolving potential issues with solar panels. With fuzzy logic, it is possible to account for uncertainties and variations in the data, while recursive least squares optimization allows for iterative adjustments of the model parameters to achieve more reliable results. This integrated approach could prove to be very effective in diagnosing and resolving solar panel issues with greater precision and efficiency.
Firstly, start with the formatting of the page. The paper should be prepared using A4 paper format with the Monitoring systems are essential for maintaining optimal performance of photovoltaic systems. A crucial aspect of these monitoring systems is fault diagnostic techniques. Fault detection and diagnostic techniques involve identifying causes that affect real-time energy production and/or the proper functioning of photovoltaic systems.
Supervision of photovoltaic systems involves comparing forecasted data with measured results from the installation and providing technical reports. These systems primarily consist of sensors (electrical and environmental), a data acquisition system with appropriate communication protocols,

and data analysis algorithms [4–35].
In recent years, the field of photovoltaic installation monitoring has matured, with an increasing number of scientific articles related to these systems emerging. Most of them address aspects of the monitoring system, such as sensors and data acquisition [7–36].
Other research works have focused on measurement instrumentation, data acquisition and storage systems, as well as system supervision methods [5, 6]. Additionally, some elements have been used to develop algorithms dedicated to PV module diagnostics and prognosis [6, 7]. Furthermore; data analysis methods for PV systems are presented in [8]. New diagnostic techniques have been proposed to monitor photovoltaic installations, predict malfunctions, and improve system performance.
Some of these photovoltaic fault detection algorithms are based on simulating the electrical circuit of the photovoltaic generator [9, 10]. Others use approaches based on electrical signals [11, 12] or various maximum power point tracking (MPPT) techniques [13, 14, 37, 38].
In this work, we are primarily interested in diagnosing faults at the photovoltaic generator level, leading to reduced production. The objective is to propose an intelligent approach using recursive least squares optimization of fuzzy logic as a solution, while taking the fewest possible measurements to meet economic constraints.
Recent solutions for the intelligent diagnosis of solar panels incorporate several innovative approaches. First, machine learning, particularly algorithms like random forests and neural networks, is increasingly used to detect faults, providing accurate and effective analyses [30]. Additionally, the integration of IoT sensors allows for real-time monitoring of panel performance, facilitating early detection of anomalies [31–39].
Furthermore, fuzzy logic systems demonstrate high efficiency in managing uncertainty in performance data, enhancing the reliability of diagnostics [32, 33, 35**?** –40]. Thermal imaging is also recognized as a promising technique for identifying physical defects on panels [**?**]. Finally, the application of genetic algorithms and other optimization methods contributes to strengthening diagnostic models, making the process more robust [34–41]. These advancements open new perspectives for the efficiency and sustainability of photovoltaic systems.
Our work based on the intelligent method integrated with fuzzy logic makes several important contributions to solar panel diagnostics. It enhances diagnostic accuracy by better handling uncertainties and imprecise data, allowing for more precise fault identification. This method enables real-time diagnostics, reducing downtime and avoiding energy losses. It also supports adaptive learning, continuously improving fault detection.
Additionally, fuzzy logic helps address ambiguous situations and variable conditions, reducing both false positives and false negatives. It facilitates proactive maintenance by detecting potential issues early, thereby optimizing energy production and return on investment. Finally, this method allows for finer data interpretation and reduces maintenance costs by preventing major faults and targeting necessary repairs.

2. Methodology

The architecture of a MAMDANI-type fuzzy inference system can be mathematically decomposed as follows:
Each input variable (x_i) is associated with a fuzzy set (A_i) defined by membership functions $\mu A_i(x_i)$, where $\mu A_i(x_i)$ gives the degree to which (x_i) belongs to the set (x_i).
For each input value (x_i), the degree of its membership in each fuzzy set is calculated using the corresponding membership functions.
For a rule R_j of the form:
If x_1 is A_1 AND x_2 is A_2 AND...THEN y is B_j its degree of activation (α_j) is calculated using the T-norm operator.
In the context of adapting fuzzy logic with the recursive least squares method, it is necessary to describe the three characteristics of a fuzzy subset. From such a function, several characteristics of the fuzzy subset can be studied: Kernel, Support, and Height (Fig. 1).

- The $Cor(A)$, is the set of all the elements which totally belong to it of the form:

$$Cor(A) = \{x \in X \mid \mu_A(x) = 1\} \tag{1}$$

- The support of a fuzzy subset A of X, denoted $Supp(A)$, is the set of all the elements which belong to it at least a little:

$$Supp(A) = \{x \in X \mid \mu_A(x) > 0\} \tag{2}$$

- The height of a fuzzy subset A of X, denoted $H(A)$, is the maximum value reached on the support of A:

$$H(A) = Sup\{\mu_A(x) \mid x \in X\} \tag{3}$$

We will then say that a fuzzy subset is normalized if its height $H(A)$ is equal to 1.
The premises of the rules are defined by the fuzzy membership to prototypes $C^{(i)}$ which are characterized by a center $\mu^{(i)}$ and a covariance matrix $\sum^{(i)}$. The degree of fuzzy membership $\beta^{(i)}(X)$ is calculated by a basis function hyper-ellipsoidal radial, as a function of the Mahalanobis distance $d_{\sum^{(i)}}(X,\mu^{(i)})$ between X and $C^{(i)}$:

$$\beta^{(i)}(X) = \frac{1}{1+d_{\sum^{(i)}}(X,\mu^{(i)})} \tag{4}$$

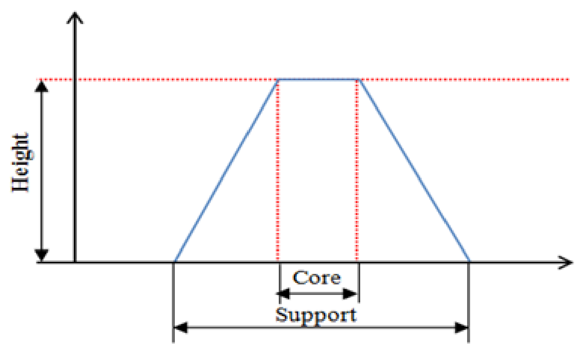

Figure 1. Characteristics of a fuzzy set of core support height.

The conclusions of the rules give the fuzzy membership to the different classes; these degrees of membership are obtained by linear functions of the inputs:

$$\hat{Y}^{(i)}(X) = (l_1^{(i)}(X);\ldots;l_C^{(i)}(X)) \tag{5}$$

where $l_C^{(i)}(X)$ represents the linear consequence function of rule (i) for class (k):

$$l_k^{(i)}(X) = \theta_k^{(i)T}X = \theta_{k,1}^{(i)}x_1 + \ldots + \theta_{k,n}^{(i)}x_n \tag{6}$$

We calculate the output of the system for each class using sum-product fuzzy inference:

$$\hat{Y}(X) = \sum_{i=1}^{r} \beta^{(i)}(X)\cdot\hat{Y}^{(i)}(X) \tag{7}$$

where (r) represents the number of fuzzy rules. Class (X) is chosen as the label corresponding to the maximum component of the system output $\hat{Y}(X) = (\hat{y}_1(X);\ldots;\hat{y}_C(X))$.

$$Classe(X) = \arg\max \hat{y}_k(X) \quad k = 1,\ldots,C \tag{8}$$

In learning consequences in fuzzy logic, we can use the Recursive Least Squares (RLS) method by activating the rules [10].
Let $\Theta^{(i)}$ be the matrix of all the parameters of the linear consequences of rule(i):

$$\Theta^{(i)} = \begin{bmatrix} \theta_{1,1}^{(i)} & \cdots & \theta_{1,C}^{(i)} \\ \vdots & \ddots & \vdots \\ \theta_{n,1}^{(i)} & \cdots & \theta_{n,C}^{(i)} \end{bmatrix} \tag{9}$$

where (C) represent the number of classes, and (n) the size of the feature vector. These matrices can be recursively learned:

$$\begin{aligned} &\theta_t^{(i)} = \Theta_{t-1}^{(i)} + P_t^{(i)}X_t\beta^{(i)}(Y_t - X_t^T\Theta_{t-1}^{(i)}); \\ &\Theta_0^{(i)} = 0 \end{aligned} \tag{10}$$

where the covariance matrix $P^{(i)} = (\sum_{k=1}^{t} X_k\cdot X_k^T)^{-1}$ is also updated recursively:

$$P_t^{(i)} = P_{t-1}^{(i)} - \frac{P_{t-1}^{(i)}X_tX_t^TP_{t-1}^{(i)}}{\frac{1}{\beta^{(i)}(X_t)} + X_t^TP_{t-1}^{(i)}X_t} \tag{11}$$

When the number of training data increases, the changes made to the conclusions by the RLS algorithm will be small, Indeed, the weight given to each piece of data being equivalent, the more the number of pieces of data increases, the lower the weight of each individual piece of data.
This property is illustrated by the fact that the covariance matrix decreases with time: $(P_t < P_{t-1})$ It is said that the gain of the algorithm tends towards zero. This property has the effect of reducing the responsiveness of the system over time. It is therefore necessary to limit the weight of old data, in other words to introduce forgetting into the recursive least squares algorithm, to maintain the learning capabilities of the system. To do this, we must work on the covariance matrix which represents the distribution of data in the recursive least squares algorithm. The principle of forgetting is to introduce a temporal update of this matrix [11]:

$$\bar{P}_t = f(P_t) \tag{12}$$

In the case of a system with slow variation over time, we introduce a forgetting factor which has the effect of giving more weight to recent data and exponentially forgetting old data. By introducing this factor, the recursive algorithm becomes:

$$\begin{aligned} P_t &= (\sum_{k=1}^{t} \lambda^{t-k}\cdot X_k\cdot X_k^T)^{-1} \\ &= (\lambda^{t-k}X_1^TX_1 + \ldots + \lambda X_{t-1}^TX_{t-1} + X_t^Tx_t)^{-1} \end{aligned} \tag{13}$$

Or in a recursive way:

$$P_t^{-1} = \lambda P_{t-1}^{-1} + X_t^TX_t;\ \ 0 < \lambda < 1 \tag{14}$$

where (λ) the forgetting factor value
This exponential weighting of the data results in the forgetting function:

$$f(P) = \frac{P}{\lambda} \tag{15}$$

The MCR adjusts the (θ) parameters continuously based on new data. Parameter updating is performed using the following equations:
Kaman's gain:

$$K(k) = P(k-1)X^T(k)[X(k)P(k-1)X^T(k) + \sigma^2 I]^{-1} \tag{16}$$

where $K(k)$ is the Kalman gain $P(k-1)$, is the error covariance matrix of the previous estimate σ^2, is the error variance, and (I) is the identity matrix.
To estimate the parameters we calculate:

$$\theta(k) = \theta(k-1) + K(k)[y(k) - X(k)\theta(k-1)] \tag{17}$$

Then the update of the covariance matrix will be:

$$P(k) = [I - K(k)X(k)]P(k-1) \tag{18}$$

After updating, diagnostic errors (prediction error) are calculated by comparing the actual observations to the fitted model predictions.

$$e(k) = y(k) - X(k)\theta(k) \tag{19}$$

To integrate fuzzy logic, we define fuzzy variables representing the different ranges of values for the detected anomalies. The variables include terms such as "low", "medium", and "high" for the severity of anomalies.

- Fuzzy membership functions are defined for each variable, such as a membership function for the prediction error will be:

$$\mu_{\text{weak}}(e) = \exp\left(-\frac{e^2}{2\sigma^2}\right) \tag{20}$$

where σ is a parameter defining the scope of the function. This detailed diagram (Fig. 2) provides a comprehensive

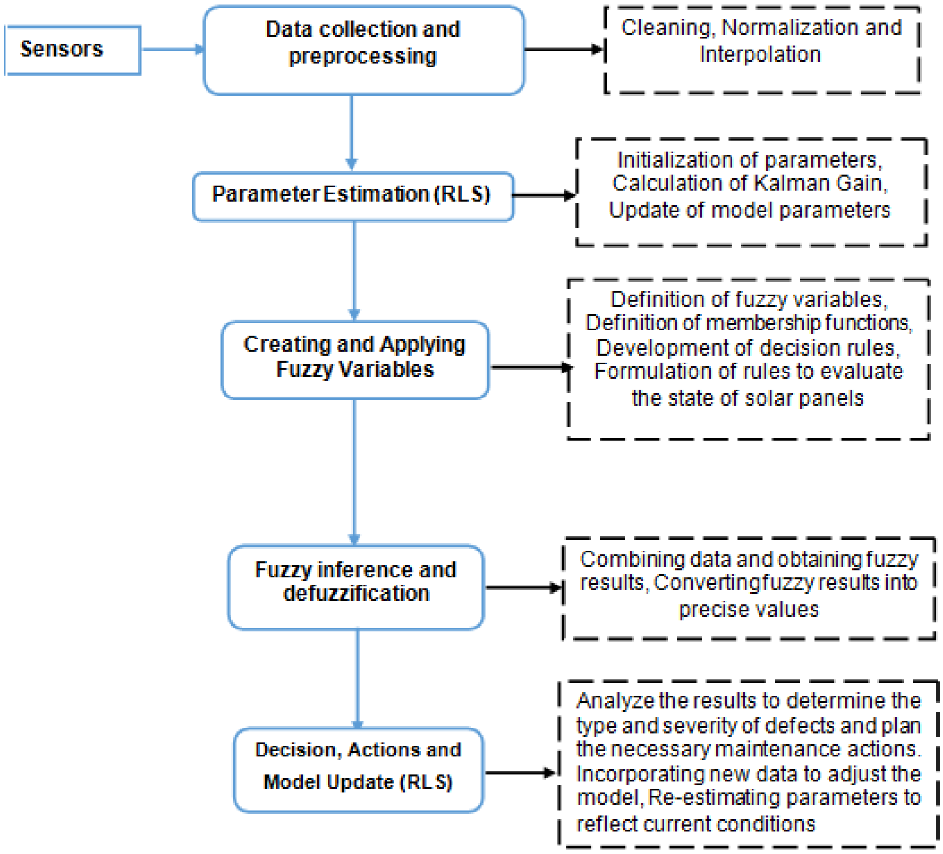

Figure 2. Intelligent recursive least squares diagram for diagnosing a solar panel.

view of the solar panel diagnostic process using the integration of Recursive Least Squares (RLS) method with fuzzy logic, enabling effective management of the performance and faults of photovoltaic systems.

We can translate the execution steps of the recursive least squares algorithm by the diagram presented in Fig. 3. The recursive least squares (RLS) algorithm which is used in step 5 of the above algorithm is presented by equations

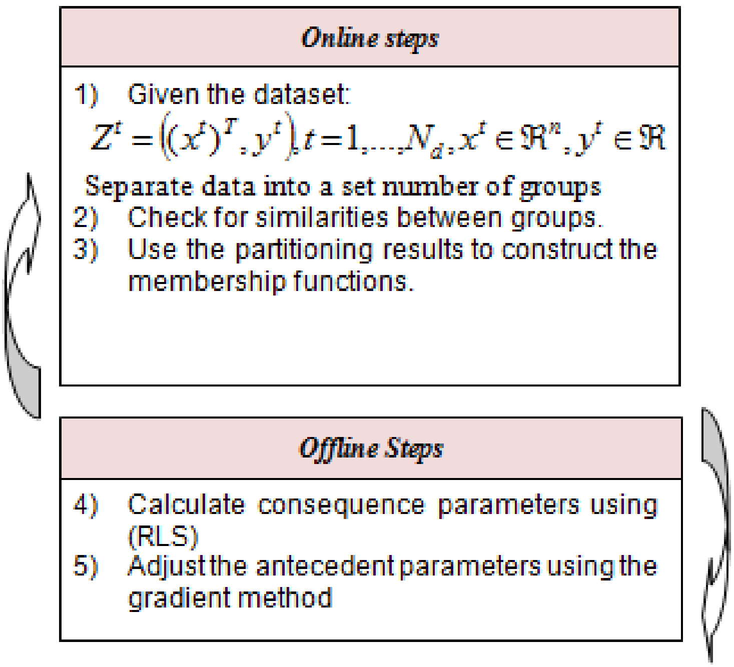

Figure 3. RLS algorithm.

[33]:

$$\begin{aligned}
\hat{\theta}(t) &= \hat{\theta}(t-1) + K_t(y(t) - x(t)^T\hat{\theta}(t-1)) \\
K_t &= \frac{P_{t-1}x(t)^T}{(\lambda I + x(t)P_{t-1}x(t)^T)} \\
P_t &= (P_{t-1} - K_t x(t) P_{t-1})\frac{1}{\lambda}
\end{aligned} \tag{21}$$

To illustrate the mathematical progression (Fig. 2) of the steps in integrating the Recursive Least Square (RLS) method with fuzzy logic, we will detail the calculations and mathematical concepts involved in each step.

- Step 1: Separate the Data into a Determined Number of Groups
  We apply a clustering method to partition the data into distinct groups.
  We choose (k) random centroids for the clusters. For each data point (x_i), we calculate the distance to the centroid (μ_j) of each Cluster Point Allocation:

$$d_{ij} = \|x_i - \mu_j\| \tag{22}$$

We assign each point to the cluster with the minimum distance:

$$C_i = \arg\min_j d_{ij} \tag{23}$$

For the Centroids Update, taking the average of the assigned points:

$$\mu_j = \frac{1}{|C_j|}\sum_{x_i \in C_j} x_i \tag{24}$$

Iterate until convergence (i.e. until the centroids no longer change significantly).

- Step 2: Check for Similarities Between Group
  We analyze the relationships between groups using two-sided similarity measures:

- The distance between Centroids:

$$d_{ik} = \|\mu_j - \mu_k\| \tag{25}$$

- The analysis of Overlaps (Fuzzy Clustering), for fuzzy clustering (fuzzy c-means), we calculated the degree of membership μ_{ij} of a poin (x_i) to the cluster (j):

$$\mu_{ij} = \frac{1}{\sum_{k=1}^{k}\left(\frac{\|x_i-\mu_j\|}{\|x_i-\mu_k\|}\right)^{\frac{2}{m-1}}} \tag{26}$$

where (m) the fuzzy parameter.

- Step 3: Construct the Membership Functions
  We previously defined the fuzzy membership functions for each group. We use Triangular functions, based on the clustering results.

- Step 4: Calculate the Consequence Parameters with RLS

■ The objective is to estimate the consequence parameters of the fuzzy rules using the RLS algorithm from the cost function:

$$J(\theta) = \sum_{i=1}^{n}(y_i - \hat{y}_i)^2 \tag{27}$$

where (y_i) the real is value and $(\hat{y}_i)$ is the value predicted by the fuzzy model.
■ For the estimation of the parameters (θ) we update the parameters using the RLS algorithm:

$$P_{k+1} = \frac{1}{\lambda}\left(P_k - \frac{K_k x_k^T P_k}{\lambda + x_k^T P_k x_k}\right) \tag{28}$$

$$K_k = \frac{P_k x_k}{\lambda + x_k^T P_k x_k} \tag{29}$$

$$\hat{\theta}_{k+1} = \hat{\theta}_k + K_k(y_k - x_k^T\hat{\theta}_k) \tag{30}$$

where λ is the forgetting factor.

- Step 5: Adjusting the antecedent parameters with the gradient method
  The objective is to optimize the antecedent parameters of the fuzzy rules using the mean squared error gradient descent method:

$$E(\theta) = \frac{1}{n}\sum_{i=1}^{n}(y_i - \hat{y}_i)^2 \tag{31}$$

where $(\hat{y}_i)$ is the output predicted by the fuzzy model.
■ The calculation of gradients of $E(\theta)$ with respect to parameter (θ) will be:

$$\frac{\partial E(\theta)}{\partial \theta_j} = -\frac{2}{n}\sum_{i=1}^{n}(y_i - \hat{y}_i)\frac{\partial \hat{y}_i}{\partial \theta_j} \tag{32}$$

■ To calculate the Parameter Update using the gradient descent rule:

$$\theta_j^{\text{new}} = \theta_j^{\text{old}} - \eta\frac{\partial E(\theta)}{\partial \theta_j} \tag{33}$$

where η is the learning rate.
This mathematical path provides an understanding of the calculations and mathematical processes involved in integrating RLS with fuzzy logic for solar panel diagnostics.

3. Fuzzy system architecture adapted by RLS

A solar panel diagnostic system based on fuzzy logic could have several steps, each associated with fuzzy rules. The general block diagram for diagnosing a solar panel based on fuzzy logic:
This is the phase of combining the results of the rules to obtain an overall fuzzy distribution for each output variable (the state of the solar panel). This may involve the use of operators such as maximization. This is usually done using Defuzzification methods such as center of gravity.

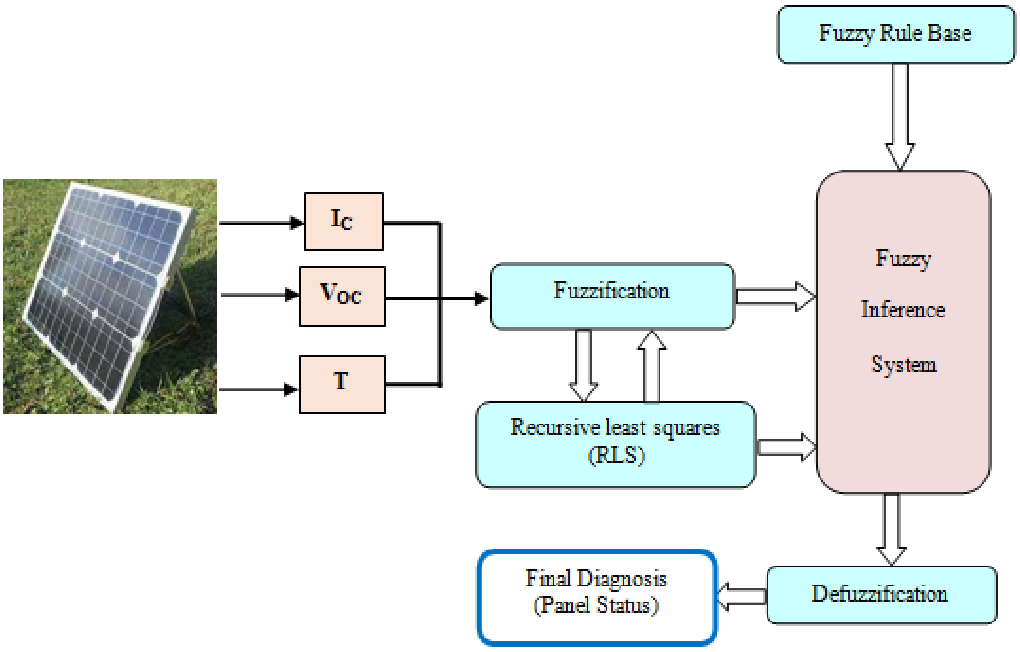

Figure 4. Confused methodology: fuzzy logic for PV diagnosis.

4. Defects encountered in the study panel

(PV BPSX3190B)
In our work we will use the BP SX3190B PV panel. The solar panel is made up of four blocks in series, i.e. 50 cells of poly-crystalline technology (Fig. 5).
Standard laboratory test conditions must have a radiation of 1000 W/m^2 and a temperature of 25 °C. The electrical characteristics of this panel are summarized in the Table 1.
The electrical characteristics of the panel are obtained with STC (Standard Test Conditions), i.e. with luminance set at 1000 W/m^2 and temperature at 25 °C. The following figures (Fig. 6, 7 and 8) show the change caused by increasing the series resistance on current, voltage and power energy.

5. Design of fuzzy logic descriptor

5.1 Voltage/current measurement

This technique is based on measurements of electrical signals, which are voltage and current [22]. Hirata et al., (2011) developed a diagnostic function which makes it possible to obtain the I (V) curves of PV modules in the same branch to automatically detect certain failures [22, 23]. Kaplan is et al., (2011) calculated form factor (FF), series and parallel resistances from the I (V) curve [26].
In this figure is a graphical curve of voltage (V) which varies with time (in minutes) in the solar panel. We note that the voltage value begins to gradually increase from the beginning of the experiment until reaching the value of 13.01 V at 11:30 a.m., then decreases and begins to rise another woman until reaching its value the highest, which is 14.21 V at 3:55 p.m. It decreases until it stabilizes gradually due to the natural changes of the solar panels.
In this curve it represents a graphical curve of the current (A) which varies with time (in minutes) in the solar panel. As the current value is low in the first few minutes, then we notice that the current value starts to increase from 9:10 a.m. until 5:02 p.m., which reaches the highest value of 2.66 A and then gradually decreases until stabilize.

Figure 5. Solar panel solar panel (Algerian region).

Table 1. Electrical characteristics of the BP SX3190B PV panel in standard conditions.

Features	Values
Open circuit voltage V_{OC}	30.6 V
Voltage V_{mp}	24.3 V
Current I_{mp}	7.82 A
Current I_{SC}	8.6 A
Maximum power at PPM P_{max}	190.26 W/Crete
Temperature Current coefficients I_{SC}	0.1 %/°C
Temperature voltage coefficients V_{OC}	−0.33 %/°C
Number of cells	50

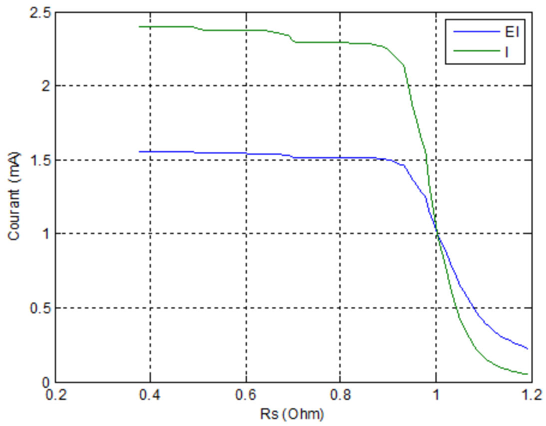

Figure 6. Current energy from increasing Rs.

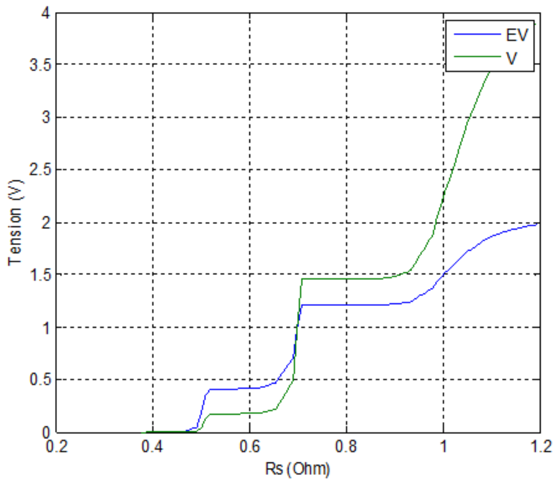

Figure 7. Voltage energy from increasing Rs.

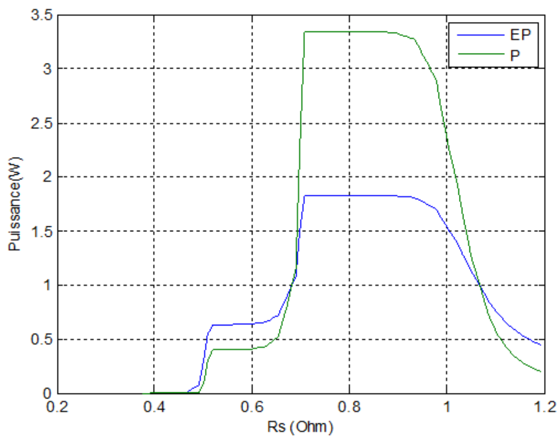

Figure 8. Power energy from increasing Rs.

5.2 Power loss analysis

The analysis of power losses in the PV system amounts to determining the power losses which are calculated by comparing the measured data to the simulated results. Chouder et al. (2010), proposed detection, supervision and fault method based on power loss analyzes [25]. Silvestre et al. (2013) used voltage and current ratios in the fault detection algorithm by measuring the losses captured in a PV system

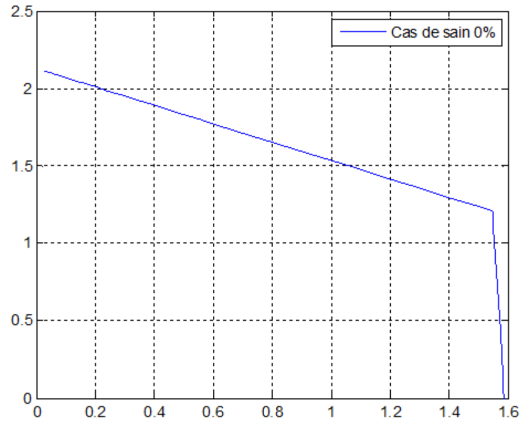

Figure 9. The measured electrical quantities (I and V) at the PV output for 0% healthy case.

[26].

5.3 Temperature-based models and heat exchange

This technique is based on the fact that faults that appear in the PV generator cause a change in the temperature of the PV module. Hu et al., (2013) and Vergura et al., (2012) modeled the physical defects of different types of PV cells using the limited element method [27–29]. It is based on the thermal behavior of PV cells resulting from electrical failures.

The curve represents the study of the variations in the temperature of the solar panels in the importance of time, as we notice that the temperature starts at around 33.91 degrees Celsius at 8 a.m., then begins to rise gradually until reaching its highest value of 52.74 degrees Celsius in 1 hour 15 hours 45 minutes, then gradually decreases until it reaches a value of 40 degrees Celsius at 6 p.m.

The fuzzy logic diagnostician is designed according to the link between the parameters which represent the factors influencing the state of the solar panel: Solar current intensity (I_{SC}), Solar panel voltage (V_{OC}) and Solar panel temperature. There are a total of 3 input variables.

The functional diagram of the fuzzy logic diagnostician is presented in figure 10 and a Mamdani type fuzzy logic

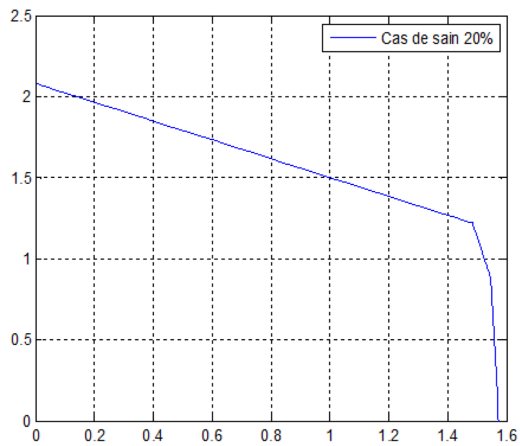

Figure 10. The measured electrical quantities (I and V) at the PV output for the case of 20% shading.

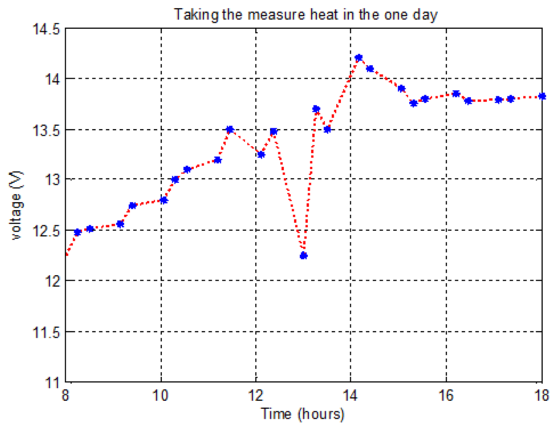

Figure 11. Tacking the measure (voltage) heat in the one day.

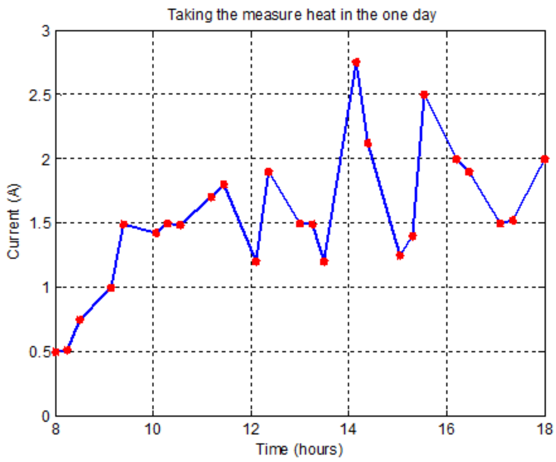

Figure 12. Tacking the measure (Current) heat in the one day.

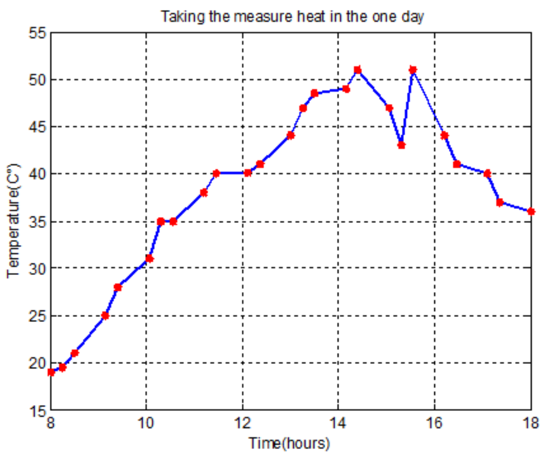

Figure 13. Tacking the measure (Temperature) heat in the one day

system was used.

Both triangular and trapezoidal shapes are used for the membership function of inputs and outputs. The centroid method is used for defuzzification. Fuzzy Logic Diagnostic is developed using Matlab Toolkit and Fuzzy Logic. The system is tested using Simulink.

To build a fuzzy diagnostic system, we used the following fuzzy logic system:

– The inputs of this system are: maximum power of the

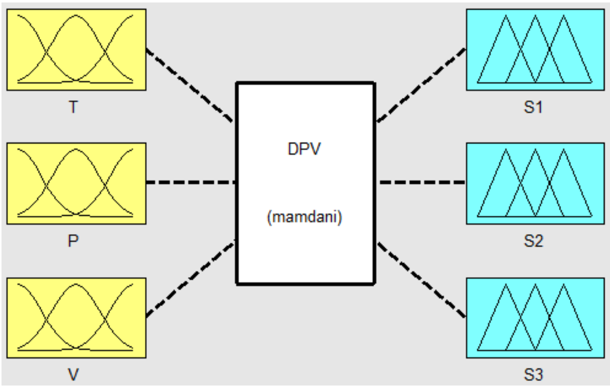

Figure 14. The fuzzy diagnostic system used with three inputs and three outputs.

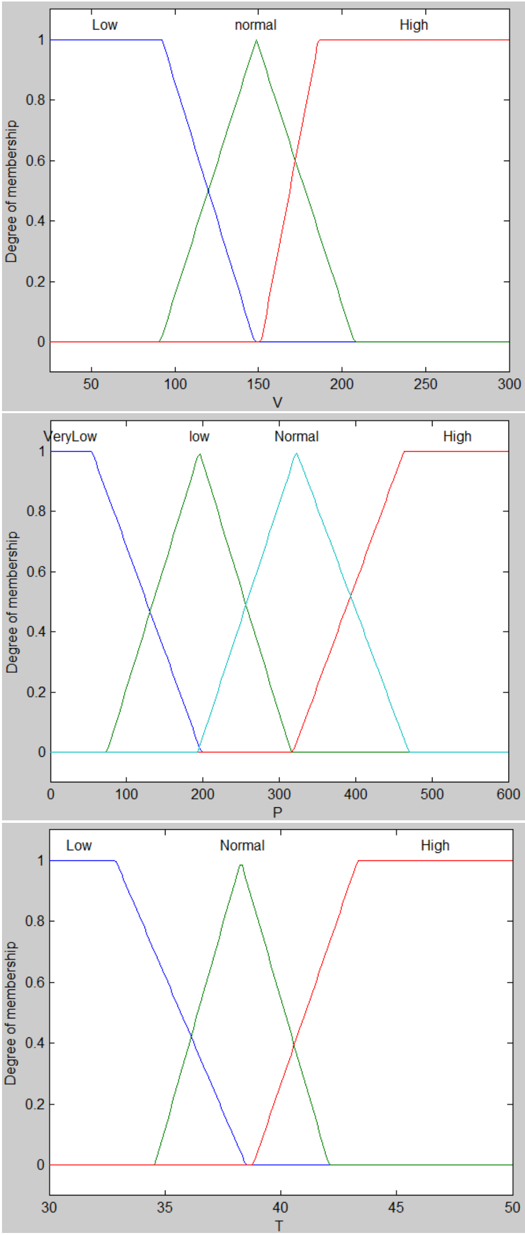

Figure 15. Fuzzy logic membership functions (inputs); (a) Voltage membership function, (b) Power membership function, (c) Temperature membership function.

module (PPM), the open circuit voltage of the module V_{OC}) and the temperature (T).

– The outputs of our fuzzy diagnostic system are: S1 between 0 and 1, S2 between 1 and 2, S3 between 2 and 3.

Following an exhaustive simulation with the variation of the input variables (T, P, and V) of the PV module, we have brought together the results obtained in the Table 2.
This section presents the simulation results of our photovoltaic system, as well as the performance of the proposed diagnostic technique. The simulation results are obtained using the MATLAB/Simulink software under the following climatic conditions (in the healthy state): Solar irradiation $G = 1000$ W/m^2 and temperature $T = 25$ °C.

Figure 16 shows the simulation results of diagnosis and detection of three different states in a photovoltaic system by the Fuzzy Logic type method, in which, at each step, the PV case is well illustrated.
The outputs of the fuzzy diagnostician are shown in detail in figure 16. The three panel states were selected as S1 for good panel status, S3 for medium and S2 for poor panel status.
Through the fuzzy surface (figure 18) and the extent of flatness and the state of curvature, we notice that the temperature factor plays a crucial role in evaluating the performance of solar panels and shows that the temperature is important in relation to the state of the electric current and the voltage generated by the solar cells as the efficiency of solar cells is linked to the temperature (As the temperature increases, the

Table 2. Variation of the three considered symptoms of the PV module.

Rule	T (°C)	P (W)	V_{OC} (V)	State 1	State 2	State 3
1	38	332	156	0.28	1.72	2.72
2	38	414	156	0.56	1.7	2.71
3	34.1	259	215	0.24	1.51	2.7
4	39.2	405	244	0.53	1.7	2.7
5	40.8	405	244	0.5	1.68	2.68
6	42.3	405	244	0.5	1.5	2.5
7	43.8	405	244	0.5	1.5	2.5
8	45	405	244	0.5	1.5	2.5
9	45	177	102	0.273	1.3	2.27
10	47.4	177	102	0.273	1.3	2.27
11	47.4	432	223	0.5	1.5	2.5
12	38	432	223	0.617	1.71	2.71
13	38	495	248	0.708	1.72	2.72
14	38	223	252	0.231	1.36	2.71
15	40.2	223	252	0.248	1.41	2.7
16	43.8	223	252	0.5	1.5	2.5
17	45	223	252	0.5	1.5	2.5
18	48	377	194	0.5	1.5	2.5

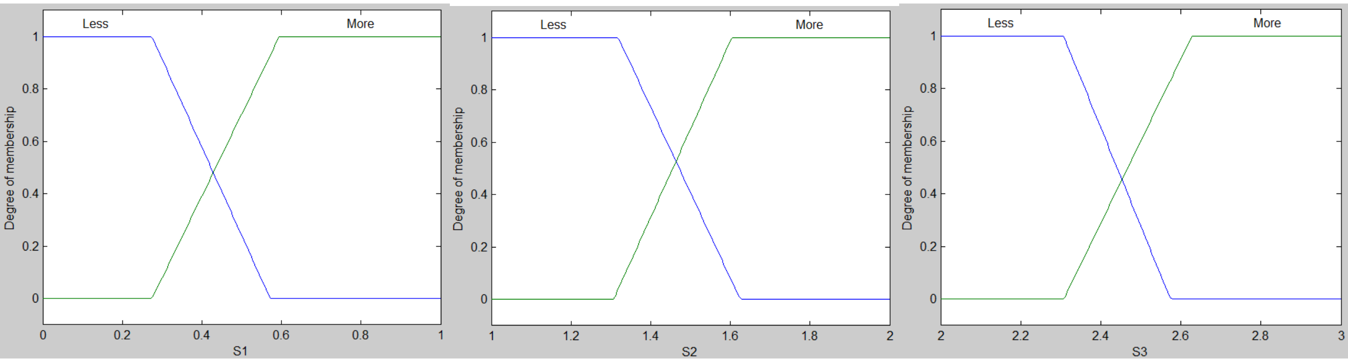

Figure 16. Fuzzy logic membership functions (Outputs); (a) First state membership function, (b) Membership function of second state, (c) Third state membership function.

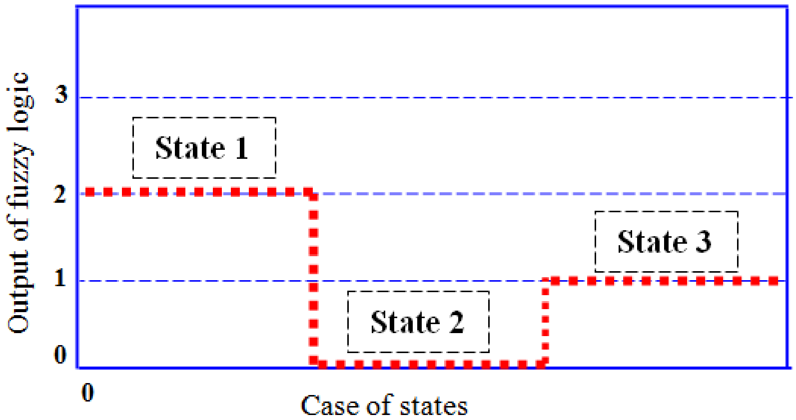

Figure 17. The result of the solar panel description.

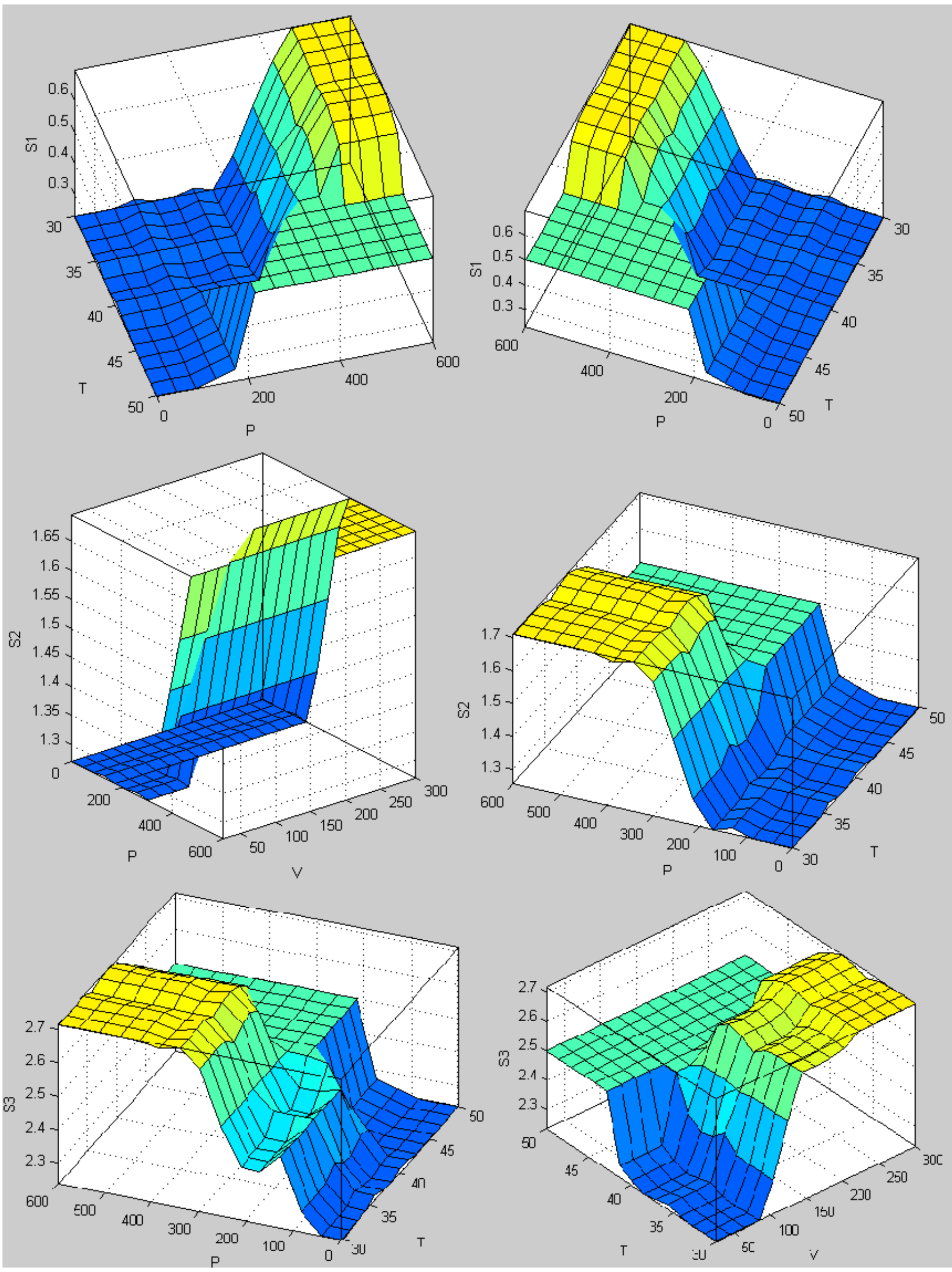

Figure 18. Fuzzy control surfaces; (a) Fuzzy control surface S1 (T, P), (b) Fuzzy control surface S1 (P, T), (c) Fuzzy control surface S2 (P, V), (d) Fuzzy control surface S2 (P, T), (e) Fuzzy control surface S3 (P, T), (f) Fuzzy control surface S3 (T, V).

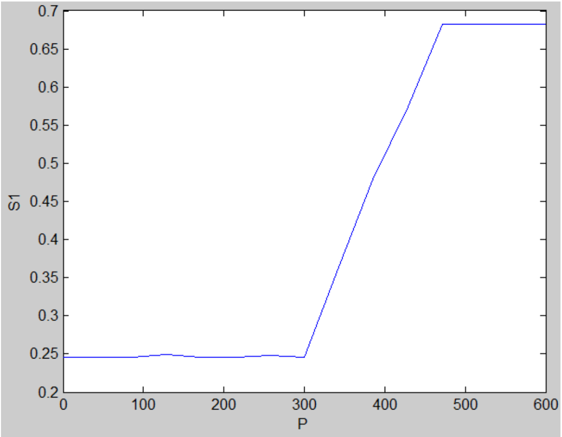

Figure 19. The fuzzy logic control output of the power.

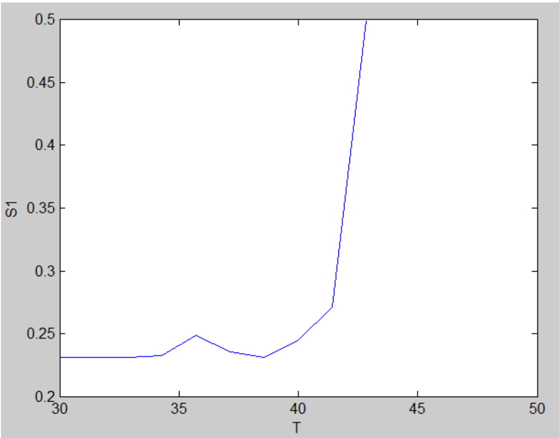

Figure 20. The fuzzy temperature control output.

performance of the cells tends to decrease. This is due to an increase in the internal resistance of the cell, leading to an increase in voltage loss and a reduction in output current), the quality and ability of solar systems to produce energy. It is important to monitor temperature to ensure stable performance of solar panels over time. By understanding the impact of temperature on the performance of solar cells, necessary steps can be taken to improve their performance and reduce heat-related deterioration.

In the figures (figure 19 and 20) we observe that the relationship between temperature and power in a solar panel is inversely proportional: when the temperature increases, the output power of the panel decreases, and vice versa. This is due to the sensitivity of photovoltaic cells to heat, which affects their efficiency in converting solar energy into electricity.

6. Quality indices of fuzzy partitions and the recursive adaptation factor

From figures 22 and 23, the difference between the two approaches (fuzzy logic and fuzzy logic adapted by the recursive least square method) in terms of correlation and regression becomes clear to us.

Which means that the effectiveness of the recursive approach in fuzzy logic.

After figure (Fig. 24), it is observed that the recursive fuzzy method smooths the data and reduces variations compared to the classic fuzzy method. This is due to the adaptive and smoothing nature of the recursive method, which allows it to better handle fluctuations and noise in the data.

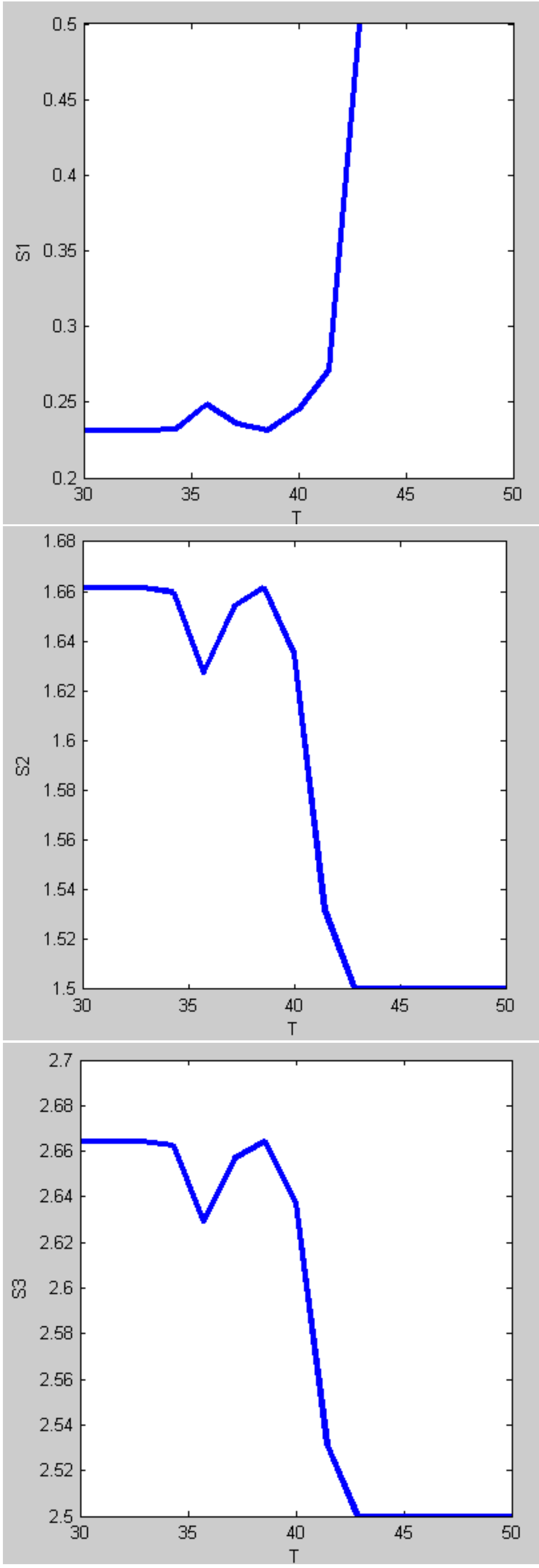

Figure 21. (a) The fuzzy (S1) control output, (b) The fuzzy (S2) control output, (c) The fuzzy (S3) control output

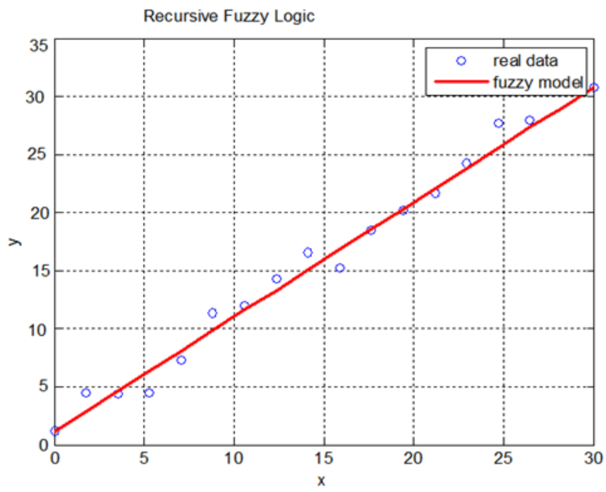

Figure 22. The recursive fuzzy approach.

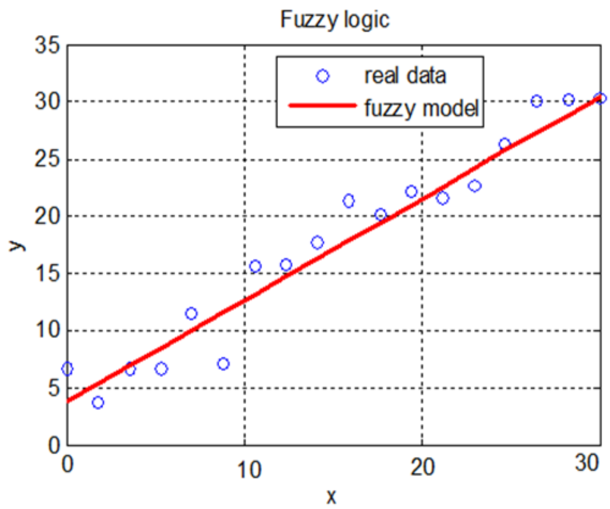

Figure 23. The normal fuzzy approach.

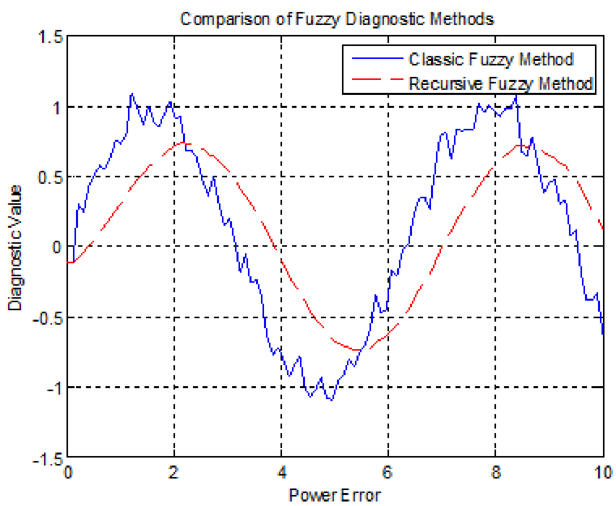

Fig. 24.Comparison of fuzzy diagnostic methods

Figure 24. Comparison of fuzzy diagnostic methods.

7. Conclusion

Solar systems play a crucial role in the transition to renewable energy, reducing our dependence on fossil fuels and mitigating the effects of climate change. The application of fuzzy logic in solar panel diagnostics represents a promising approach to improving the reliability and efficiency of these systems by accounting for the complex and variable nature of the data. The study presented demonstrates the effectiveness of this method, supported by convincing results from several case studies, enabling rapid and accurate problem identification and promoting proactive maintenance. The integration of fuzzy logic with the recursive least squares method constitutes a notable innovation, providing robust evaluation even with incomplete or noisy data. However, this approach has limitations, such as its complexity, sensitivity to outliers, and challenges related to parameter tuning and result interpretation. Looking ahead, promising prospects include the development of machine learning algorithms to refine fuzzy logic, the exploration of combinations with other techniques like neural networks, and the extension of this method to large-scale solar installations, paving the way for new approaches to managing sustainable energy infrastructures.

Nomenclature

Abbreviations	Definition of the term
x_i	Variable
A_i	Input variable
$\mu A_i(x_i)$	The membership functions of (A_i)
$l_C^{(i)}(X)$	The linear consequence function
$\hat{Y}$	System output
R_j	Fuzzy logic rules
α_j	Degree of activation
$P^{(i)}$	The covariance matrix
λ	The forgetting factor value
RLS	Recursive least squares
V_{OC}	Open circuit voltage
$P_{\max}$	Maximum power at PPM
I_{SC}	Short circuit current
STC	Testing Standard Conditions
T	Temperature (°C)
P_t	The recursive algorithm

Authors contributions
Authors have contributed equally in preparing and writing the manuscript.

Availability of data and materials
The data that support the findings of this study are available from the corresponding author upon reasonable request.

Conflict of interests
The authors declare that they have no known competing financial interests or personal relationships that could have appeared to influence the work reported in this paper.

References

[1] Power FS. Global market outlook. 2016. URL http://www.solarpowereurope.org.

[2] A. Triki-lahiani, A. B. Abdelghani, and I. Slama-belkhodja. "**Fault Detection and Monitoring Systems for Photovoltaic Installations: A Review**.". *Renewable Sustainable Energy Review*, pages 0–1, 2017.
DOI: https://doi.org/10.1016/j.rser.2017.09.101.

[3] L. Bun. "**Detection et localisation de defauts dans un systeme photovoltaïque**.". *Hal-Id, Detection et Localisation de Defauts pour un Systeme PV*, 2012. URL https://theses.hal.science/tel-00647189v1.

[4] G. Ball, B. Brooks, J. Johnson, A. Rosenthal, M. Albers, and T. Zgonena. "**Inverter Ground-Fault Detection Blind Spot**.". *Mitigation Methods', Prepared by Solar America Board for Codes and Standards*.
DOI: https://doi.org/10.13140/RG.2.1.3836.8720.

[5] D. L. King, M. A. Quintana, J. A. Kratochvil, D. E. Ellibee, and B. R. Hansen. "**Photovoltaic Module Performance and Durability Following Long-term**.". *Field Exposure*, page 241–56, 2000.
DOI: https://doi.org/10.1002/(SICI)1099-159X(200003/04)8:2.

[6] J. Han, J. D. Jeong, I. Lee, and S. H. Kim. "**Low-Cost Monitoring of Photovoltaic Systems at Panel Level in Residential Homes Based on Power Line Communication**.". *IEEE Transactions on Consumer Electronics*, pages 441–425, 2017.
DOI: https://doi.org/10.3390/fr12050881.

[7] I. Cristaldi, G. Leone, and S. Vergura. "**Performance Index of Photovoltaic Fields for Diagnostic Purposes**.". 2016.
DOI: https://doi.org/10.1049/cp.2016.0556.

[8] S. R. Madeti and S. N. Singh. "**A comprehensive study on different types of faults and detection techniques for solar photovoltaic system**.". *Solar Energy*, 158:161–185, 2017.
DOI: https://doi.org/10.1016/j.solener.2017.08.069.

[9] A. Mellit, G. M. Tina, and S. A. Kalogirou. "**Fault detection and diagnosis methods for photovoltaic systems: a review**.". *Renewable Sustainable Energy Review*, 91:1–17, 2018.
DOI: https://doi.org/10.1016/j.rser.2018.03.062.

[10] E. Garoudja, F. Harrou, Y. Sun, K. Kara, A. Chouder, and S. Silvestre. "**Statistical fault detection in photovoltaic systems**.". *Solar Energy*, 150:485–499, 2017.
DOI: https://doi.org/10.1016/j.solener.2017.04.043.

[11] Y. Hirata, S. Noro, T. Aoki, and S. Miyazawa. "**Diagnosis Photovoltaic Failure by Simple Function Method to Acquire I-V Curve of Photovoltaic Modules String**.". 2011.
DOI: https://doi.org/10.1109/PVSC.2008.4922833.

[12] B. Çak. "**A novel voltage-current characteristic based global maximum power point tracking algorithm in photovoltaic systems**.". page 112, 2016.
DOI: https://doi.org/10.1016/j.energy.2016.05.121.

[13] N. Aouchiche, M. Becherif, A. HadjArab, M. S. Aitcheikh, H. S. Ramadan, and A. Cheknane. "**Dynamic Performance Comparison for MPPT-PV Systems using Hybrid Pspice/Matlab Simulation**.". *Int J Emerg Electr Power Syst*, 17:529–39, 2016.
DOI: https://doi.org/10.1515/ijeeps-2016-0074.

[14] N. Bizon. "**Global Extremum Seeking Control of the power generated by a Photovoltaic Array under Partially Shaded Conditions**.". *Energy Conversion Management*, 109:71–85, 2016.
DOI: https://doi.org/10.1016/j.enconman.2015.11.046.

[15] B.-M. Bernadette. "**Logique floue, principes, aide a la décision**.". *Lavoisier*, 2003. URL https://hal.science/hal-01533303.

[16] G. Kamingu. Théorie des ensembles flous, lareq one pager. *Buildings*, 11(1):37–45, . URL http://www.lamsade.dauphine.fr/mcda/biblio/Category/thesis.html.

[17] P. Angelov and X. Zhou. "**Evolving fuzzy-rule-based classifiers from data streams**.". *Fuzzy Systems, IEEE Transactions*, 16(6): 1462–1475, 2008.
DOI: https://doi.org/10.1109/TFUZZ.2008.925904.

[18] E. Lughofer and P. Angelov. "**Handling drifts and shifts in online data streams withe volving fuzzy systems**.". *Applied Soft Computing*, 11(2):2057–2068, 2011.
DOI: https://doi.org/10.1016/j.asoc.2010.07.003.

[19] L. M. Karmacharya and R. Gokaraju. "**Fault Location in Ungrounded Photovoltaic System Using Wavelets and ANN**.". *IEEE Trans. Power Del.*, 33(2):549–559, 2018.
DOI: https://doi.org/10.1109/TPWRD.2017.2721903.

[20] L. Chen and X. Wang. "**Adaptive fault localization in photovoltaic systems**.". *IEEE Trans. Smart Grid*, 9(6):6752–6763, 2018.
DOI: https://doi.org/10.1109/TSG.2017.2722821.

[21] L. A. Zadeh. "**Fuzzy sets, fuzzy loqic and fuzzy systems**.".
DOI: https://doi.org/10.1142/2895.

[22] Y. Liu, M. Li, X. Ji, X. Luo, M. Wang, and Y. Zhang. "**A comparative study of the maximum power point tracking methods for PV systems**.". *Energy and Conversion Management*, 85:809–816, 2014.
DOI: https://doi.org/10.1016/j.enconman.2014.01.049.

[23] T. Zhou and W. Sun. "**Study on maximum power point tracking of photovoltaic array in irregular shadow**.". *International Journal of Electric Power Energy System*, 66:227–234, 2015.
DOI: https://doi.org/10.1016/j.ijepes.2014.10.030.

[24] S. Nema, R. K. Nema, and G. Agnihotri. "**MATLAB/Simulink based study of photovoltaic cells/modules/array and their experimental verification**.". *International journal of Energy and Environment*, 1(3):487–500, 2010. URL https://www.researchgate.net/publication/44024846_Matlab_simulink_based_study_of_photovoltaic_cells_modules_array_and_their_experimental_verification.

[25] Johnson et al. "**Photovoltaic DC arc fault detector testing at Sandia National Laboratories**.". *Conf. Rec. IEEE Photovolt. Spec. Conf.*, pages 003614–003619, 2011.
DOI: https://doi.org/10.1109/PVSC.2011.6185930.

[26] G. Kamingu. "**Théorie des ensembles flous**.". *Lareq One Pager*, 11 (1):37–45, .
DOI: https://doi.org/10.13140/RG.2.2.31700.81286.

[27] E. Lughofer and P. Angelov. "**Handling drifts and shifts in online data streams withe volving fuzzy systems**.". *Applied Soft Computing*, 11(2):2057–2068, 2011.
DOI: https://doi.org/10.1016/j.asoc.2010.07.003.

[28] Y. Sun, A. Chouder, S. Silvestre, E. Garoudja, K. Kara, and F. Harrou. "**Statistical fault detection in photovoltaic systems**.". *Sol. Energy*, 150:485–499, 2017.
DOI: https://doi.org/10.1016/j.solener.2017.04.043.

[29] R. Araneo and S. Celozzi. "**Transient behavior of wind towers grounding systems under lightning strikes**.". *Int J Energy Environ Eng*, 2015.
DOI: https://doi.org/10.1007/s40095-015-0196-7.

[30] J. A. Smith et al. "**Enhancing solar power forecasting accuracy using machine learning**.". *Renewable Energy*, 2022.
DOI: https://doi.org/10.1016/j.csite.2024.104924.

[31] H. Kim and D. Lee. "**Probabilistic Solar Power Forecasting Based on Bivariate Conditional Solar Irradiation Distributions**.". *IEEE Transactions on Sustainable Energy*, 12(4):2031–2041, 2021.
DOI: https://doi.org/10.1109/TSTE.2021.3077001.

[32] B. Pratap, P. Sharma, L. K. Patel, A. T. Singh, S. N. Oulkar, and M. Thamban. "**Surface melting of a debris-covered glacier and its geomorphological control—A case study from Batal Glacier, western Himalaya"**.". *Geomorphology. Elsevier.*, 2023.
DOI: https://doi.org/10.1016/j.geomorph.2023.108686.

[33] P. Lopez, S. Cristina, E. Lucchi, and G. Franco. "**ACCEPTANCE OF BUILDING INTEGRATED PHOTOVOLTAIC (BIPV) IN HERITAGE BUILDINGS AND LANDSCAPES: POTENTIALS, BARRIER AND ASSESSMENT CRITERIA**.". *Construction Pathology, Rehabilitation Technology and Heritage Management*, 2020. URL http://repository.supsi.ch/id/eprint/12136.

[34] Y. Wang et al. "**Long short-term memory networks for solar irradiance prediction**.". *Solar Energy*, 222:41–49, 2021.
DOI: https://doi.org/10.1109/LGRS.2021.3107139.

[35] N. Priyadarshi, P. Kiran Maroti, F. Azam, and M. G. Hussien. "**An improved Z-source inverter-based sensorless induction motor-driven photovoltaic water pumping with Takagi–Sugeno fuzzy MPPT**.". *IET Renewable Power Generation. IET Renew. Power Gener.*, pages 1–14, 2022.
DOI: https://doi.org/10.1049/rpg2.12654.

[36] N. Priyadarshi, S. Padmanaban, J. Bo Holm-Nielsen, F. Blaabjerg, and M. Sagar Bhaskar. "**An Experimental Estimation of Hybrid ANFIS–PSO-Based MPPT for PV Grid Integration UNDER Fluctuating Sun Irradiance**.". *IEEE Systems Journal*, 2019.
DOI: https://doi.org/10.1109/JSYST.2019.2949083.

[37] N. Priyadarshi, S. Padmanaban, M. S. Bhaskar, F. Azam, Baseem Khan, and M. G. Hussien. "**A novel hybrid grey wolf optimized fuzzy logic control based photovoltaic water pumping system**.". *IET Renewable Power Generation. IET Renew. Power Gener.*, pages 1–12, 2022.
DOI: https://doi.org/10.1049/rpg2.12638.

[38] N. Priyadarshi, S. Padmanaban, M. S. Bhaskar, F. Azam, I. B. M. Taha, and M. G. Hussien. "**An adaptive TS-fuzzy model based RBF neural network learning for grid integrated photovoltaic applications**.". *IET Renewable Power Generation*, .
DOI: https://doi.org/10.1049/rpg2.12505.

[39] N. Priyadarshi, S. Padmanaban, M. S. Bhaskar, and Baseem Khan. "**An experimental performance verification of continuous mixed P-norm based adaptive asymmetrical fuzzy logic controller for single stage photovoltaic grid integration**.". *IET Renewable Power Generation*, .
DOI: https://doi.org/10.1049/rpg2.12410.

[40] N. Priyadarshi, P. Kiran Maroti, and Baseem Khan. "**An adaptive grid integrated photovoltaic system with perturb T–S fuzzy based sliding mode controller MPPT tracker: An experimental realization**.". *IET Renewable Power Generation*, .
DOI: https://doi.org/10.1049/rpg2.12738.

[41] A. Singh Chauhan, R. Singh, N. Priyadarshi, B. Twala, S. Suthar, and S. Swami. "**Unleashing the power of advanced technologies for revolutionary medical imaging: pioneering the healthcare frontier with artificial intelligence**.". *Discover Artificial Intelligence*, 2024.
DOI: https://doi.org/10.1007/s44163-024-00161-0.